

Detecting the Neutrino Gravitational Wave Memory from Core-Collapse Supernovae using the Moon

KIRANJYOT GILL¹

¹Center for Astrophysics | Harvard & Smithsonian, 60 Garden Street, Cambridge, MA 02138-1516, USA

Submitted to ApJ Letters

ABSTRACT

Following the milestone of detecting gravitational waves (GWs) from merging compact binaries, the next significant watershed moment in GW astronomy lies in detecting GWs from core-collapse supernovae (CCSNe). In this *Letter*, I describe the possibility of detecting the *GW linear memory* – a phenomenon resulting from a combination of aspherical matter ejection and anisotropic neutrino emission during stellar collapse using GW detectors on the Moon. This would grant unprecedented access to the sub- Hz/ Hz GW frequency range, which is inaccessible to current and future terrestrial GW detectors. I demonstrate that three-dimensional CCSNe model matter and neutrino GW waveforms may be detectable by both seismometer and interferometric lunar GW detectors, with the latter design proposal extending 10 kpc to megaparsec detection distances.

Keywords: core-collapse supernovae, gravitational waves, neutrinos, lunar gravitational wave detectors

1. INTRODUCTION

The birth of gravitational wave (GW) astronomy began when binary black hole (BBH) mergers were first detected (Abbott et al. 2016), and the prowess of multi-messenger GW astronomy was showcased through the inaugural observation of a binary neutron star (BNS) merger (Abbott et al. 2017; Soares-Santos et al. 2017). Nevertheless, one eagerly anticipated source of GWs still remains undiscovered. Core-collapse supernovae (CCSNe), heralding the death of stars with initial masses exceeding $8M_{\odot}$, remain an alluring GW detection prospect. Past three-dimensional simulations (see Burrows & Vartanyan 2021; Mezzacappa 2023 for recent reviews) suggest that during core collapse and subsequent core bounce at super-nuclear densities, hot fluid instabilities emerge within the newly-formed proto-neutron star (PNS) and within the developing cavity between the PNS surface and the SN shock wave (Morozova et al. 2018; Radice et al. 2019; Powell & Müller 2019; Andresen et al. 2019; Mezzacappa et al. 2020; Vartanyan et al. 2023). Such an asymmetric explosion perturbs the PNS sufficiently, through time-varying quadrupolar motions, to generate GWs at frequencies between \sim few Hz to a few kHz (Kuroda et al. 2016; Janka et al. 2016; Andresen et al. 2017; Morozova et al. 2018; Andresen et al. 2019; Powell & Müller 2019; Radice et al. 2019; Burrows & Vartanyan 2021; Mezzacappa 2023; Vartanyan et al. 2023).

The additional anisotropic emission of neutrinos (Motizuki et al. 2004; Kotake et al. 2004; Takiwaki & Kotake 2018), combined with the aspherical, large-scale motion of ejected matter, gives rise to sub- Hz GW emission. This induces a seconds-long lasting alteration in the space-time metric, which shows a secular time evolution that does not average to zero (Epstein 1978; Burrows et al. 1995; Burrows & Hayes 1996; Mueller & Janka 1997; Kotake et al. 2007, 2009a,b, 2011; Müller et al. 2012; Richardson et al. 2022; Vartanyan et al. 2023), and persists beyond the cessation of neutrino emission post shock breakout. This effect, known as the *GW linear memory*, bears the stamp of important explosion asymmetries and possible neutron star formation. Although the high-frequency GW emission may reach strain values of a few centimeters at most (Morozova et al. 2018; Powell & Müller 2019; Andresen et al. 2019), the low-frequency component instead may reach several $\sim 10^2$ centimeters (Vartanyan et al. 2019; Vartanyan & Burrows 2020; Vartanyan

Corresponding author: Kiranjyot Gill;
 jasmine.gill@cfa.harvard.edu

et al. 2022, 2023). However, due to the squared frequency dependence of the GW energy, E_{GW} , the total emitted GW energy is still much smaller compared to that from compact binary mergers. E_{GW} from CCSNe ranges anywhere from $\sim 10^{-11}$ to $10^{-8} \text{ M}_\odot \text{c}^2$ and is contingent on certain characteristics of the progenitor (Kuroda et al. 2016; Andresen et al. 2017; Kuroda et al. 2017; Morozova et al. 2018; Radice et al. 2019; Powell & Müller 2019; Andresen et al. 2019; Vartanyan et al. 2019; Powell & Müller 2020; Andresen et al. 2021; Vartanyan et al. 2022, 2023; Mezzacappa et al. 2023).

GW emission originating from slowly-rotating, massive progenitors likely composes the majority of the local CCSNe GW source population within 20 Mpc (Heger et al. 2005). Due to the squared frequency dependence of the GW energy, E_{GW} , the total emitted GW energy is still much smaller compared to that from compact binary mergers. E_{GW} from CCSNe ranges anywhere from $\sim 10^{-11}$ to $10^{-8} \text{ M}_\odot \text{c}^2$ and is contingent on certain characteristics of the progenitor (Kuroda et al. 2016; Andresen et al. 2017; Kuroda et al. 2017; Morozova et al. 2018; Radice et al. 2019; Powell & Müller 2019; Andresen et al. 2019; Vartanyan et al. 2019; Powell & Müller 2020; Andresen et al. 2021; Vartanyan et al. 2022, 2023; Mezzacappa et al. 2023). Using terrestrial GW detectors, such as LIGO (LIGO Scientific Collaboration et al. 2015), detection capabilities for GW emission from non/slowly-rotating CCSNe are limited to our Galaxy, with distances within 10 kiloparsecs (Gossan et al. 2016; Abbott et al. 2016; Abbott et al. 2020; Szczepański et al. 2021). Additionally, the low-frequency GW memory emission would not be observable within the sensitivity band of advanced LIGO (LIGO Scientific Collaboration et al. 2015) or its terrestrial successors (Reitze et al. 2019; Sathyaprakash et al. 2012; Maggiore et al. 2020), nor would it be accessible with space-based detectors such as LISA (Amaro-Seoane et al. 2017; Colpi et al. 2024).

GW detectors on the Moon offer a potential solution by bridging this gap (Jani & Loeb 2021; Harms et al. 2021; LILA 2023; Ajith et al. 2024) and granting access to the sub- Hz/ Hz GW frequency spectrum. Seismically, the Moon is exceptionally quiet (Harms 2022), and its permanently shadowed regions are cold ($< 100 \text{ K}$) and thermally stable (Cozzumbo et al. 2023), making the lunar environment an ideal setting for regularized GW detections. There are two primary GW lunar detector proposals of interest. The first involves a terrestrial-inspired GW detector (Jani & Loeb 2021; LILA 2023), which is able to be deployed in a triangular configuration separated by tens of kilometers straddling the edge of a large lunar crater (such as the Shoemaker crater near the southern lunar pole (Basilevsky & Li 2024)). The second proposal (Harms et al. 2021; Ajith et al. 2024) instead focuses on using an array of inertial sensors to monitor the lunar surface's vibrational response to GWs with a lower frequency limit of 0.1 Hz that is set by the lowest order quadrupole moment of the Moon. Either design proposal would access frequencies below traditional, next generation terrestrial GW detector noise floors ($\leq 10 \text{ Hz}$) and above the detector noise floor of LISA ($\geq 0.1 \text{ Hz}$).

In this *Letter*, I demonstrate that neutrino-driven CCSNe model waveforms, specifically their low frequency emission due to the GW linear memory, may be detectable out to a few megaparsecs using lunar GW detectors. In Section §2, I discuss the matter and neutrino GW strains from three-dimensional CCSNe models possessing GW linear memory. I then extend and taper all GW signals out to 10 seconds and back down to zero. I then project these time-extended GW CCSNe strains against the noise amplitudes of current (LIGO Scientific Collaboration et al. 2015) and future (Sathyaprakash et al. 2012; Reitze et al. 2019; Maggiore et al. 2020) generation terrestrial GW detectors and first-generation lunar GW detector configurations (Jani & Loeb 2021; LILA 2023; Ajith et al. 2024). I discuss the improved detection prospects with lunar GW detectors subsequently conclude in Section §3.

2. EXTENDED CORE-COLLAPSE SUPERNOVAE GRAVITATIONAL WAVE MODELS

I use a neutrino-driven waveform model from Vartanyan et al. (2023), as summarized in Table 1. These 9 waveform models span a range of progenitor star parameters, physical approximations, and signal properties. The GW model duration is defined as the time span from the onset of collapse until the end of the simulation.

Vartanyan et al. 2023 introduces several progenitor models spanning from $9 - 23 \text{ M}_\odot$ and are currently the longest three-dimensional core-collapse simulations performed to date. All models demonstrate early prompt convection, along with a haze of GW emission, extending from $\sim 300 \text{ Hz} - 2 \text{ kHz}$ around $\sim 0.2 - 1.5 \text{ s}$ due to the accretion plumes ringing off the PNS that induce g/f-modal oscillations. The total GW emissions vary by as much as three orders of magnitude across different progenitors. They also observe the emergence of the GW linear memory effect due to neutrino emission anisotropy, peaking at frequencies of 25 Hz, with larger amplitudes on smaller timescales. Both the 11 and 23 M_\odot models exhibit amplified GW strains due to the cumulative effect of neutrino GW linear memory. Conversely, their models showed a general correlation where the lower mass progenitors tend to possess smaller effects from GW linear memory and overall smaller amplitudes. Furthermore, the neutrino anisotropy continues to influence

Table 1. GW Waveform Model from Select Neutrino-Driven CCSNe Simulation

Waveform Model	Progenitor Mass	Duration	E_{GW}	GW Features
	(M_{\odot})	(s)	($10^{-10} M_{\odot}c^2$)	
Vartanyan et al. 2023 (V23)	9a, 9b, 9.25, 9.50 11, 12.25, 14, 15.01, 23	1.76, 2.04, 2.79, 2.14 4.46, 2.05, 2.53, 3.79, 6.14	0.22, 0.30, 2.46, 4.95 45.27, 30.90, 59.18, 107.58, 166.17	f-/g-modes, SASI, convection, linear memory

NOTE—For each waveform, I provide the associated progenitor masses, signal duration, the emitted GW energy, and the dominant GW signal features present. The f-/g-modes refer to the respective fundamental and gravity mode oscillations associated with the PNS.

the GW strain beyond the conclusion of the longest model run. This underscores the significance of neutrino emission asymmetry, which intensifies by at least two orders of magnitude within 50 ms. However, it's crucial to note that for every progenitor model, late-time neutrino-sourced GW energies, although increasing, remain more than two orders of magnitude smaller than their matter counterparts.

2.1. GW Waveform Extension and Tapering Function

Although the longest simulations extend to approximately four seconds post-bounce, they still lack duration of at least ten seconds to effectively constrain the 0.1 - 1 Hz frequency region. I overcome this limitation by artificially extending all GW signals to ten seconds in order to reach 0.1 Hz. By doing this, I allow the estimates of the GW linear memory from dominant, anisotropic neutrino processes (Arca Sedda et al. 2020; Vartanyan & Burrows 2020; Vartanyan et al. 2023) into the frequency regime that would be accessible only through lunar GW observatories. I adopt the waveform extension and tapering function found in (Richardson et al. 2022) and use the extension function defined as,

$$h_{\times/+}^e(t_e) = h_{\times/+}^N + \frac{2G}{c^4 R} \alpha_{\times/+}^c \int_N^{t_e} C \tau^{-n}(\tau) d\tau = h_{\times/+}^N + \frac{2G}{c^4 R} \frac{\alpha_{\times/+}^c C}{1-n} (t_e^{1-n} - N^{1-n}) \quad (1)$$

where the subscript $\times/+$ denotes the cross and plus polarization modes and the notation $h_{\times/+}^N$ refers to the GW signal at the specific time N corresponding to the time of shutdown of neutrino transport within the CCSN simulation. $\alpha_{\times/+}^c$ denotes the constant parameters representing neutrino anisotropy, t_e represents times post neutrino transport shutdown (where $t < N$), and C is a constant determined to ensure consistency between the analytically extended neutrino luminosity and its pre-transport shutdown values (expressed in units of $\text{s}^n \text{ergs}$). Lastly, n is varied between 0.9 and 1.1, approximating the cooling phase of the PNS.

Additionally, if the amplitude of the GW signal is non-zero at the time of simulation truncation, the abrupt jump from some finite value to zero will induce artifacts within the GW signal. To account for this, I taper the GW signals with the tapering function from (Richardson et al. 2022) that brings the GW signal back to zero,

$$h_{\times/+}^{\text{tail}} = \frac{h_{\times/+}^{\text{end}}}{2} [1 + \cos(2\pi f_t (t - t^{\text{end}}))] \quad (2)$$

where f_t is the frequency of the tapering function, t^{end} is the duration of the simulation (10 s), h^{end} represents the signal value at t^{end} , and f_t is the frequency of the tapering function.

3. LUNAR GRAVITATIONAL WAVE DETECTION PROSPECTS

Figure 1 shows the resulting matter and neutrino sourced GW spectra, $2\sqrt{f}|\tilde{h}(f)|$, from core-collapse explosions of varying stellar masses at 10 kpc against the noise curves for the Lunar Gravitational Wave Antenna (LGWA) (Harms et al. 2021), the Gravitational-wave Lunar Observatory for Cosmology (GLOC) (Jani & Loeb 2021), and the Laser Interferometer Lunar Antenna (LILA) (LILA 2023). The noise curve from LIGO O3 (Livingston) is included in grey for comparison, along with noise curves from Cosmic Explorer Maggiore et al. (2020) and Einstein Telescope (Reitze et al. 2019). In order to understand the detection volume given a detector noise floor, the matched filter signal-to-noise ratio (SNR) is calculated, as shown in Table 2,

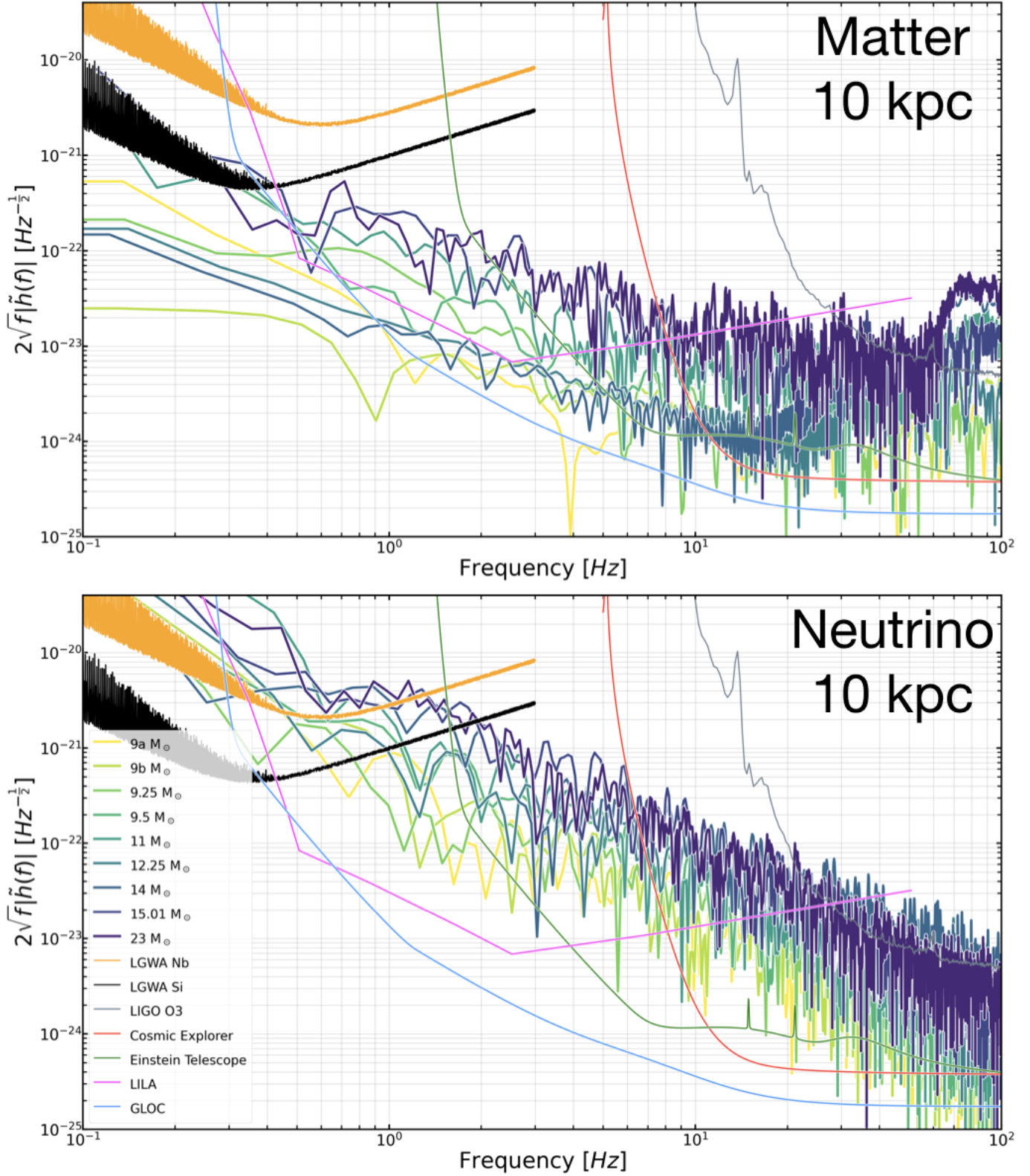


Figure 1. The gravitational wave spectra, $2\sqrt{f}|\tilde{h}(f)|$, associated with extended GW models injected at 10 kpc projected against terrestrial and lunar detector noise curves, $\sqrt{S_n}$. The Figure is split according to the respective matter and neutrino GW strains for the V23 models. Notably, there exists a substantial disparity of several orders of magnitude between the strains sourced by these mechanisms, with the neutrino-driven GW strain surpassing the matter-driven counterpart in signal strength. Additionally, the bounce seen in the higher frequencies in the matter GW strain is primarily due to the modal oscillations generated by the PNS.

Table 2. The total, cumulative signal-to-noise ratios for different CCSNe waveform models at 10 kpc.

Progenitor Model	Matter sourced GW strain						Neutrino sourced GW strain						
	M_{\odot}	LIGO O3	CE	ET	LGWA	LILA	GLOC	LIGO O3	CE	ET	LGWA	LILA	GLOC
9a	11	150	240	< 1	4.6	320		11	150	240	4.1	76	2600
9b	15	210	220	< 1	160	450		16	210	220	8.0	85	2600
9.25	20	290	3700	< 1	1.7	600		20	290	3700	15	130	2400
9.50	33	480	450	< 1	10	1000		33	480	450	11	94	2500
11	60	960	840	3.2	60	2100		60	960	840	250	4100	110000
12.25	32	480	440	-	< 1	970		32	480	440	53	2800	25000
14	55	800	740	-	8.4	1700		56	800	740	51	1200	23000
15.01	65	110	910	2.9	330	2200		66	1100	910	90	5600	2100
23	79	110	1200	1.1	17	16000		79	110	110	75	4800	5800

NOTE— The total signal-to-noise ratio (SNR) for each waveform model is presented for a detection distance of 10 kpc for both the *matter*, *neutrino* GW strains. SNRs are evaluated for the current advanced detector noise floor (O3), as well as for three different proposed lunar gravitational wave detectors. Lastly, - equates to no accumulated SNR.

$$\text{SNR} = \sqrt{4 \int_{f_{\min}}^{\infty} \frac{|\tilde{h}(f)|^2}{S_n(f)} df} \quad (3)$$

where $\tilde{h}(f)$ is the frequency domain representation of the GW strain, $S_n(f)$ is the single-sided detector noise PSD and f_{\min} is the frequency of the GW signal at the start of the sample time series.

There are a few trends to note from Figure 1 and Tables 2, 3. Firstly, the GW linear memory will not be detectable in current terrestrial interferometers, which is contrary to what is claimed by (Richardson et al. 2024), as seen by Table 3. The total SNR from a galactic CCSN situated at 10 kpc would come from the 100-1000 Hz range. However, more massive progenitors do result in larger SNRs agnostic of GW detector. For example, in the context of LILA, for a galactic CCSN at 10 kpc, the 9a matter model has an SNR of 4.5 whereas the 23 matter model has an SNR of 18. Secondly, as seen in Figure 1 and in both Tables 2 and 3, the GW strain from neutrinos does result in larger SNRs across all detectors. This is present in even the low-mass progenitor population. In the context of LILA, the 9 - 9.50 M_{\odot} neutrino models at 10 kpc possessed SNRs larger by a factor of two compared to the SNRs of the 9 - 9.50 matter models. This trend remains true even in the context of the non-exploding 12.25 and 14 M_{\odot} models that directly form a BH post collapse. Additionally, although the 12.25 and 14 M_{\odot} matter models accumulate no SNR with LGWA, the 12.25 and 14 M_{\odot} neutrino models still accumulate SNRs of ~ 50 and still may be detected out to megaparsec distances with LILA. In the context of GLOC, such models would possess SNRs of 10^2 at 10 megaparsecs. Note that both the neutrino and matter sourced GW strains would be emitted simultaneously in time. Thirdly, the choice of lunar detector design significantly impact the detection distances. Interferometer-based designs like GLOC and LILA are preferred over seismometer proposals like LGWA due to limitations at frequencies below 1 Hz, evident in Figure 1. For instance, the 15.01 M_{\odot} matter and neutrino models in LILA and GLOC exhibit galactic SNRs of 10^3 - 10^4 and SNRs of 10^2 at a few megaparsecs, contrasting with LGWA, which barely achieves SNRs of 10^2 at 10 kpc. Moreover, LGWA may be unable to detect any emissions from the low-mass stellar population.

In conclusion, the burgeoning knowledge from GW emission from CCSNe underscores the importance of realistically assessing detection capabilities for the first GW detection from CCSNe. As demonstrated in this paper, both current and future terrestrial interferometer GW detectors will be unable to detect the GW linear memory. However, interferometric lunar GW detectors like LILA and GLOC enable low-frequency GW detection from CCSNe at megaparsec distances, even for vanilla, low-mass CCSNe. Future endeavors will concentrate on establishing data analysis infrastructure for a lunar GW environment for both stellar collapse and binary merger GW signals.

Table 3. Signal-to-noise ratios produced by the GW linear memory between 0.1 and 10 Hz for CCSNe waveform models at 10 kpc.

Progenitor Model	Matter sourced GW strain						Neutrino sourced GW strain					
	M_{\odot}	LIGO O3	CE	ET	LGWA	LILA	GLOC	LIGO O3	CE	ET	LGWA	LILA
9a	-	1.9	10	< 1	4.5	35	-	< 1	2.8	4.1	73	1200
9b	-	< 1	4.4	< 1	160	13	-	< 1	3.8	7.9	84	1200
9.25	-	1.3	6.4	< 1	1.2	21	-	< 1	3.3	15	130	1200
9.50	-	10	47	< 1	10	160	-	< 1	2.3	10	85	1800
11	-	28	160	3.2	59	530	-	< 1	2.8	250	4000	46000
12.25	-	< 1	< 1	-	0.11	2.9	-	< 1	3.6	52	2800	10000
14	-	< 1	1.7	-	< 1	5.3	-	< 1	3.1	51	1150	10000
15.01	-	25	130	2.9	330	430	-	< 1	3.4	89	5500	9700
23	-	10	48	1.1	17	170	-	< 1	3.2	75	4800	4200

NOTE— The signal-to-noise ratio (SNR) contribution from the GW linear memory for each waveform model within 10 kpc for both the *matter*, *neutrino* GW strains. SNRs are evaluated for the current advanced detector noise floor (O3), as well as for three different proposed lunar gravitational wave detectors. Lastly, - equates to no accumulated SNR.

REFERENCES

Abbott, B. P., Abbott, R., Abbott, T. D., et al. 2016, *PhRvL*, 116, 061102, doi: [10.1103/PhysRevLett.116.061102](https://doi.org/10.1103/PhysRevLett.116.061102)

Abbott, B. P., et al. 2016, *Phys. Rev. D*, 94, 102001, doi: [10.1103/PhysRevD.94.102001](https://doi.org/10.1103/PhysRevD.94.102001)

Abbott, B. P., Abbott, R., Abbott, T. D., et al. 2017, *PhRvL*, 119, 161101, doi: [10.1103/PhysRevLett.119.161101](https://doi.org/10.1103/PhysRevLett.119.161101)

—. 2020, *PhRvD*, 101, 084002, doi: [10.1103/PhysRevD.101.084002](https://doi.org/10.1103/PhysRevD.101.084002)

Ajith, P., Amaro Seoane, P., Arca Sedda, M., et al. 2024, arXiv e-prints, arXiv:2404.09181, doi: [10.48550/arXiv.2404.09181](https://doi.org/10.48550/arXiv.2404.09181)

Amaro-Seoane, P., Audley, H., Babak, S., et al. 2017, arXiv e-prints, arXiv:1702.00786, doi: [10.48550/arXiv.1702.00786](https://doi.org/10.48550/arXiv.1702.00786)

Andresen, H., Glas, R., & Janka, H. T. 2021, *MNRAS*, 503, 3552, doi: [10.1093/mnras/stab675](https://doi.org/10.1093/mnras/stab675)

Andresen, H., Müller, B., Müller, E., & Janka, H.-T. 2017, *MNRAS*, 468, 2032, doi: [10.1093/mnras/stx618](https://doi.org/10.1093/mnras/stx618)

Andresen, H., Müller, E., Janka, H. T., et al. 2019, *Monthly Notices of the Royal Astronomical Society*, 486, 2238, doi: [10.1093/mnras/stz990](https://doi.org/10.1093/mnras/stz990)

Andresen, H., Müller, B., Müller, E., & Janka, H.-T. 2017, *Monthly Notices of the Royal Astronomical Society*, 468, 2032, doi: [10.1093/mnras/stx618](https://doi.org/10.1093/mnras/stx618)

Andresen, H., Müller, E., Janka, H.-T., et al. 2019, *Monthly Notices of the Royal Astronomical Society*, 486, 2238, doi: [10.1093/mnras/stz990](https://doi.org/10.1093/mnras/stz990)

Arca Sedda, M., Berry, C. P. L., Jani, K., et al. 2020, *Classical and Quantum Gravity*, 37, 215011, doi: [10.1088/1361-6382/abb5c1](https://doi.org/10.1088/1361-6382/abb5c1)

Basilevsky, A., & Li, Y. 2024, *Planetary and Space Science*, 241, 105839, doi: <https://doi.org/10.1016/j.pss.2024.105839>

Burrows, A., & Hayes, J. 1996, *PhRvL*, 76, 352, doi: [10.1103/PhysRevLett.76.352](https://doi.org/10.1103/PhysRevLett.76.352)

Burrows, A., Hayes, J., & Fryxell, B. A. 1995, *ApJ*, 450, 830, doi: [10.1086/176188](https://doi.org/10.1086/176188)

Burrows, A., & Vartanyan, D. 2021, *Nature*, 589, 29, doi: [10.1038/s41586-020-03059-w](https://doi.org/10.1038/s41586-020-03059-w)

Colpi, M., Danzmann, K., Hewitson, M., et al. 2024, arXiv e-prints, arXiv:2402.07571, doi: [10.48550/arXiv.2402.07571](https://doi.org/10.48550/arXiv.2402.07571)

Cozzumbo, A., Mestichelli, B., Mirabile, M., et al. 2023, arXiv e-prints, arXiv:2309.15160, doi: [10.48550/arXiv.2309.15160](https://doi.org/10.48550/arXiv.2309.15160)

Epstein, R. 1978, *ApJ*, 223, 1037, doi: [10.1086/156337](https://doi.org/10.1086/156337)

Gossan, S. E., Sutton, P., Stuver, A., et al. 2016, *PhRvD*, 93, 042002, doi: [10.1103/PhysRevD.93.042002](https://doi.org/10.1103/PhysRevD.93.042002)

Harms, J. 2022, *Phys. Rev. Lett.*, 129, 071102, doi: [10.1103/PhysRevLett.129.071102](https://doi.org/10.1103/PhysRevLett.129.071102)

Harms, J., Ambrosino, F., Angelini, L., et al. 2021, *The Astrophysical Journal*, 910, 1, doi: [10.3847/1538-4357/abe5a7](https://doi.org/10.3847/1538-4357/abe5a7)

Heger, A., Woosley, S. E., & Spruit, H. C. 2005, *ApJ*, 626, 350, doi: [10.1086/429868](https://doi.org/10.1086/429868)

Jani, K., & Loeb, A. 2021, *Journal of Cosmology and Astroparticle Physics*, 2021, 044, doi: [10.1088/1475-7516/2021/06/044](https://doi.org/10.1088/1475-7516/2021/06/044)

Janka, H.-T., Melson, T., & Summa, A. 2016, ArXiv e-prints. <https://arxiv.org/abs/1602.05576>

Kotake, K., Iwakami, W., Ohnishi, N., & Yamada, S. 2009a, *ApJL*, 697, L133, doi: [10.1088/0004-637X/697/2/L133](https://doi.org/10.1088/0004-637X/697/2/L133)

—. 2009b, *ApJ*, 704, 951, doi: [10.1088/0004-637X/704/2/951](https://doi.org/10.1088/0004-637X/704/2/951)

Kotake, K., Iwakami-Nakano, W., & Ohnishi, N. 2011, *ApJ*, 736, 124, doi: [10.1088/0004-637X/736/2/124](https://doi.org/10.1088/0004-637X/736/2/124)

Kotake, K., Ohnishi, N., & Yamada, S. 2007, *ApJ*, 655, 406, doi: [10.1086/509320](https://doi.org/10.1086/509320)

Kotake, K., Sawai, H., Yamada, S., & Sato, K. 2004, *The Astrophysical Journal*, 608, 391, doi: [10.1086/392530](https://doi.org/10.1086/392530)

Kuroda, T., Kotake, K., Hayama, K., & Takiwaki, T. 2017, *The Astrophysical Journal*, 851, 62, doi: [10.3847/1538-4357/aa988d](https://doi.org/10.3847/1538-4357/aa988d)

Kuroda, T., Kotake, K., & Takiwaki, T. 2016, *The Astrophysical Journal*, 829, L14, doi: [10.3847/2041-8205/829/1/l14](https://doi.org/10.3847/2041-8205/829/1/l14)

LIGO Scientific Collaboration, Aasi, J., Abbott, B. P., et al. 2015, *Classical and Quantum Gravity*, 32, 074001, doi: [10.1088/0264-9381/32/7/074001](https://doi.org/10.1088/0264-9381/32/7/074001)

LILA, C. 2023, Vanderbilt University. <https://www.vanderbilt.edu/lunarlabs/lila/>

Maggiore, M., Van Den Broeck, C., Bartolo, N., et al. 2020, *JCAP*, 2020, 050, doi: [10.1088/1475-7516/2020/03/050](https://doi.org/10.1088/1475-7516/2020/03/050)

Mezzacappa, A. 2023, *IAU Symposium*, 362, 215, doi: [10.1017/S1743921322001831](https://doi.org/10.1017/S1743921322001831)

Mezzacappa, A., Marronetti, P., Landfield, R. E., et al. 2020, *PhRvD*, 102, 023027, doi: [10.1103/PhysRevD.102.023027](https://doi.org/10.1103/PhysRevD.102.023027)

—. 2023, *PhRvD*, 107, 043008, doi: [10.1103/PhysRevD.107.043008](https://doi.org/10.1103/PhysRevD.107.043008)

Morozova, V., Radice, D., Burrows, A., & Vartanyan, D. 2018, *The Astrophysical Journal*, 861, 10, doi: [10.3847/1538-4357/aac5f1](https://doi.org/10.3847/1538-4357/aac5f1)

Motizuki, Y., Madokoro, H., & Shimizu, T. 2004, in EAS Publications Series, Vol. 11, EAS Publications Series, ed. A. Jorissen, S. Goriely, M. Rayet, L. Siess, & H. Boffin, 163–171, doi: [10.1051/eas:2004011](https://doi.org/10.1051/eas:2004011)

Mueller, E., & Janka, H. T. 1997, *A&A*, 317, 140

Müller, E., Janka, H. T., & Wongwathanarat, A. 2012, *A&A*, 537, A63, doi: [10.1051/0004-6361/201117611](https://doi.org/10.1051/0004-6361/201117611)

Powell, J., & Müller, B. 2019, *MNRAS*, 487, 1178, doi: [10.1093/mnras/stz1304](https://doi.org/10.1093/mnras/stz1304)

—. 2020, *MNRAS*, 494, 4665, doi: [10.1093/mnras/staa1048](https://doi.org/10.1093/mnras/staa1048)

Radice, D., Morozova, V., Burrows, A., Vartanyan, D., & Nagakura, H. 2019, *The Astrophysical Journal*, 876, L9, doi: [10.3847/2041-8213/ab191a](https://doi.org/10.3847/2041-8213/ab191a)

Radice, D., Morozova, V., Burrows, A., Vartanyan, D., & Nagakura, H. 2019, *ApJL*, 876, L9, doi: [10.3847/2041-8213/ab191a](https://doi.org/10.3847/2041-8213/ab191a)

Reitze, D., Adhikari, R. X., Ballmer, S., et al. 2019, in *Bulletin of the American Astronomical Society*, Vol. 51, 35. <https://arxiv.org/abs/1907.04833>

Richardson, C. J., Andresen, H., Mezzacappa, A., et al. 2024, arXiv e-prints, arXiv:2404.02131, doi: [10.48550/arXiv.2404.02131](https://doi.org/10.48550/arXiv.2404.02131)

Richardson, C. J., Zanolin, M., Andresen, H., et al. 2022, *PhRvD*, 105, 103008, doi: [10.1103/PhysRevD.105.103008](https://doi.org/10.1103/PhysRevD.105.103008)

Sathyaprakash, B., Abernathy, M., Acernese, F., et al. 2012, *Classical and Quantum Gravity*, 29, 124013, doi: [10.1088/0264-9381/29/12/124013](https://doi.org/10.1088/0264-9381/29/12/124013)

Soares-Santos, M., Holz, D. E., Annis, J., et al. 2017, *ApJL*, 848, L16, doi: [10.3847/2041-8213/aa9059](https://doi.org/10.3847/2041-8213/aa9059)

Szczepańczyk, M. J., Antelis, J. M., Benjamin, M., et al. 2021, *PhRvD*, 104, 102002, doi: [10.1103/PhysRevD.104.102002](https://doi.org/10.1103/PhysRevD.104.102002)

Takiwaki, T., & Kotake, K. 2018, *MNRAS*, 475, L91, doi: [10.1093/mnrasl/sly008](https://doi.org/10.1093/mnrasl/sly008)

Vartanyan, D., & Burrows, A. 2020, *ApJ*, 901, 108, doi: [10.3847/1538-4357/abafac](https://doi.org/10.3847/1538-4357/abafac)

Vartanyan, D., Burrows, A., & Radice, D. 2019, *MNRAS*, 489, 2227, doi: [10.1093/mnras/stz2307](https://doi.org/10.1093/mnras/stz2307)

Vartanyan, D., Burrows, A., Wang, T., Coleman, M. S. B., & White, C. J. 2023, *PhRvD*, 107, 103015, doi: [10.1103/PhysRevD.107.103015](https://doi.org/10.1103/PhysRevD.107.103015)

Vartanyan, D., Coleman, M. S. B., & Burrows, A. 2022, *MNRAS*, 510, 4689, doi: [10.1093/mnras/stab3702](https://doi.org/10.1093/mnras/stab3702)

ACKNOWLEDGEMENTS

The author thanks Avi Loeb for inspiration and Edo Berger for motivation. The author also thanks Karan Jani, David Vartanyan, and John A. Lewis for insightful and creative discussions. The author additionally thanks the CCSNe simulation community for their publicly available GW waveforms. This research has made use of data or software obtained from the Gravitational Wave Open Science Center (gw-openscience.org), a service of LIGO Laboratory, the LIGO Scientific Collaboration, the Virgo Collaboration, and KAGRA. LIGO Laboratory and Advanced LIGO are funded by the United States National Science Foundation (NSF) as well as the Science and Technology Facilities Council (STFC) of the United Kingdom, the Max-Planck-Society (MPS), and the State of Niedersachsen/Germany for support of the construction of Advanced LIGO and construction and operation of the GEO600 detector. Additional support for Advanced LIGO was provided by the Australian Research Council. Virgo is funded, through the European Gravitational Observatory (EGO), by the French Centre National de Recherche Scientifique (CNRS), the Italian Istituto Nazionale di Fisica Nucleare (INFN) and the Dutch Nikhef, with contributions by institutions from Belgium, Germany, Greece, Hungary, Ireland, Japan, Monaco, Poland, Portugal, Spain. The construction and operation of KAGRA are funded by Ministry of Education, Culture, Sports, Science and Technology (MEXT), and Japan Society for the Promotion of Science (JSPS), National Research Foundation (NRF) and Ministry of Science and ICT (MSIT) in Korea, Academia Sinica (AS) and the Ministry of Science and Technology (MoST) in Taiwan.